

Scope and Mechanism on Iridium-f-Amphamide Catalyzed Asymmetric Hydrogenation of Ketones

Zhi-Qin Liang,^a Ti-Long Yang,^a Guoxian Gu,^a Li Dang^{*,a,b} and Xumu Zhang^{*,a}

Dedicated to Professor Xiyun Lu on the occasion of his 90th birthday

ABSTRACT A series of novel and easily accessed ferrocene-based amino-phosphine-sulfonamide (f-Amphamide) ligands have been developed and applied in Ir-catalyzed asymmetric hydrogenation of aryl ketones, affording the corresponding chiral secondary alcohols with excellent results (up to >99% conversion, >99% ee and TON up to 200,000). DFT calculations suggest an activating model involving an alkali cation Li⁺.

KEYWORDS aryl ketone, asymmetric, f-Amphamide, hydrogenation, iridium

Introduction

Catalytic asymmetric hydrogenation of prochiral ketones is a convenient and economical method to prepare chiral alcohols,^[1] which are significant building blocks in pharmaceuticals and natural products.^[2] Since Noyori's milestone work in the 1990s wherein the BINAP-ruthenium-diamine catalytic system was originally developed for hydrogenation of ketones,^[3] numerous ligands including bidentate and tridentate ligands have been synthesized and investigated to access chiral alcohols via metal catalyzed asymmetric hydrogenation in the past decades.^[4]

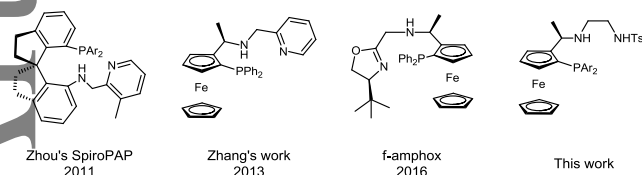


Figure 1 Selected Tridentate Ligands for Asymmetric Hydrogenation of Aryl Ketones

In terms of the tridentate PNN ligands, there are limited examples for asymmetric hydrogenation of ketones. In 2011, Zhou et al reported the tridentate spiro pyridine-aminophosphine ligands SpiroPAP for hydrogenation of ketones, giving chiral alcohols with excellent results in the iridium catalytic system (Figure 1).^[5] In 2013, Chen and Zhang's group successfully developed tridentate ferrocene-based amino-phosphine pyridine ligands for iridium-catalyzed asymmetric hydrogenation of ketones with encouraging results (Figure 1).^[6] Subsequently, our group successively developed a series of ferrocene-based tridentate ligands f-amphox^[7] (Figure 1), f-ampha^[8] and famphol^[9], which were highly efficient ligands for iridium-catalyzed asymmetric hydrogenation of ketones. Although many ligands for asymmetric hydrogenation of ketones have been developed, considering increasing industrial demand, easily accessed and practical ones are still highly desirable. Herein, we successfully developed a class of readily prepared and air-stable tridentate ferrocene-based amino-phosphine sulfonamide (f-Amphamide) ligands, which displayed excellent performance in iridium-catalyzed asymmetric hydrogenation of aryl ketones. Compared with other neutral PNN ligands, the sulfonamide is acidic (pKa~10), and the new f-Amphamide is a neutral ligand.

Results and Discussion

Results

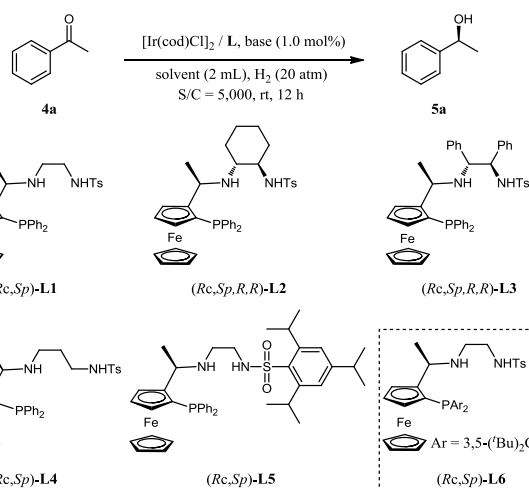
The preparation of the tridentate PNN ligand f-Amphamide is very simple. The f-Amphamide ligands **L1-L6** were efficiently prepared by a three-step manipulation from commercially available (*R*)-Ugi's amine (see in supporting information).^[10] With f-Amphamide ligands in hand, we began our research by evaluating its catalytic performance in Ir-catalyzed asymmetric hydrogenation of model substrate acetophenone **4a**. With the catalyst obtained in situ by mixing [Ir(cod)Cl]₂ and ligand **L1**, the solvent effect was investigated (S/C = 5,000). As shown in Table 1, solvent was critical to achieve high conversion and enantiocontrol. Alcohols proved to be superior to other solvents including toluene, DCM, THF etc., and *i*-PrOH turned to be the best solvent in terms of conversion and enantiocontrol (66-96% ee, Table 1, entries 1-7).

Further evaluation of different f-Amphamide ligands revealed that the structure of the amino sulfonamide had important effect on the enantioselectivity. To our surprise, **L1** and **L6** ligands with a simple sulfonamide motif gave better results (**L1**, **L6** vs **L2**, **L3**, **L4**, **L5**). The optimal ligand **L6** with two sterically hindered 3,5-di-*tert*-phenyl groups on P atom provided the hydrogenated product **5a** with full conversion and 98% ee (Table 1, entry 12). Various bases were investigated for this hydrogenation reaction catalyzed by Ir-**L6** (S/C = 5,000) in *i*-PrOH. Moderate enantioselectivities were obtained in the presence of KO^tBu, NaO^tBu, NaOH and Cs₂CO₃ (80-88% ee, >99% conversions, Table 1, entries 13-16). It revealed that LiO^tBu was the best choice for this transformation. The results retained the same level even the catalyst loading was reduced to 0.01 mol% (S/C = 10,000, Table 1, entry 17).

^a Department of Chemistry, Southern University of Science and Technology, 1088 Xueyuan Rd, Nanshan District, Shenzhen, Guangdong 518055, P. R. China. Email: zhangxm@sustc.edu.cn.

^b Department of Chemistry and Key Laboratory for Preparation and Application of Ordered Structural Materials of Guangdong Province, Shantou University, Guangdong 515063, P. R. China. Email: ldang@stu.edu.cn.

This article has been accepted for publication and undergone full peer review but has not been through the copyediting, typesetting, pagination and proofreading process, which may lead to differences between this version and the Version of Record. Please cite this article as doi: 10.1002/cjoc.201800129

Table 1 Reaction Condition Optimization with **4a**^a

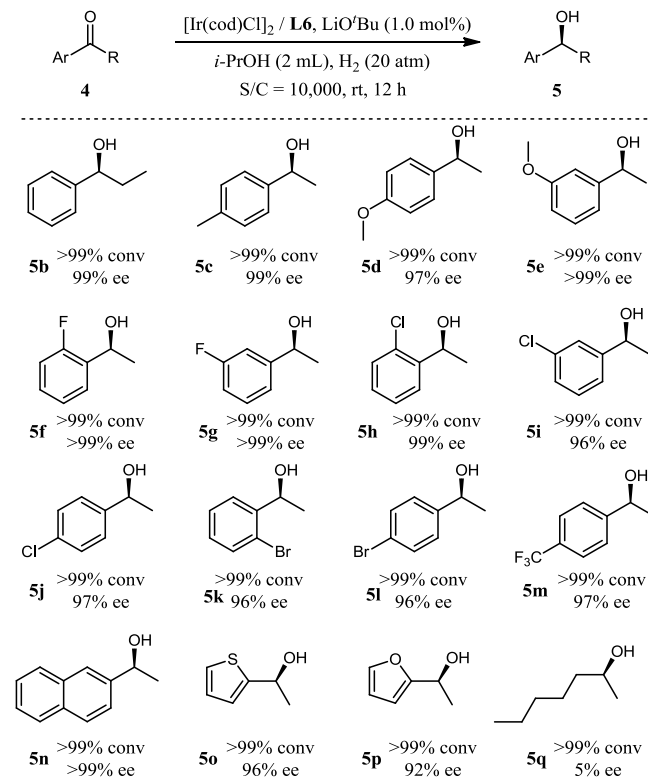
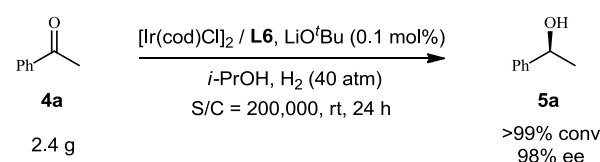
entry	ligand	solvent	base	conv. [%] ^b	ee [%] ^c
1	L1	toluene	LiO ^t Bu	22	94
2	L1	CH ₂ Cl ₂	LiO ^t Bu	5	90
3	L1	THF	LiO ^t Bu	6	75
4	L1	MeOH	LiO ^t Bu	17	66
5	L1	EtOH	LiO ^t Bu	63	93
6	L1	1,4-dioxane	LiO ^t Bu	nr	nd
7	L1	<i>i</i> -PrOH	LiO ^t Bu	>99	96
8	L2	<i>i</i> -PrOH	LiO ^t Bu	>99	83
9	L3	<i>i</i> -PrOH	LiO ^t Bu	>99	95
10	L4	<i>i</i> -PrOH	LiO ^t Bu	>99	80
11	L5	<i>i</i> -PrOH	LiO ^t Bu	>99	90
12	L6	<i>i</i> -PrOH	LiO ^t Bu	>99	98
13	L6	<i>i</i> -PrOH	KO ^t Bu	>99	80
14	L6	<i>i</i> -PrOH	NaO ^t Bu	>99	88
15	L6	<i>i</i> -PrOH	NaOH	>99	88
16	L6	<i>i</i> -PrOH	Cs ₂ CO ₃	>99	72
17 ^d	L6	<i>i</i> -PrOH	LiO ^t Bu	>99	98

^a Reaction conditions: **4a** (2.0 mmol), 0.02 mol% [Ir(cod)Cl]₂, 0.042 mol% L1, 1.0 mol% LiO^tBu, 2.0 mL solvent, room temperature. Absolute configuration determined by comparison of the optical rotation with that known in literatures. ^b Determined by ¹H NMR. ^c Determined by HPLC analysis. ^d S/C=10,000.

Under the optimal conditions (Ir/L6, 20 atm H₂/1.0 mol% LiO^tBu, S/C = 10,000, rt), the substrate scope was then investigated. As depicted in Scheme 1, all of aryl alkyl ketones were transformed smoothly, providing the corresponding chiral alcohols in quantitative conversions with 92–99% ee. The substrates bearing either an electron-donating (Me, MeO) or electron-withdrawing group (F, Cl, Br, CF₃) on the phenyl ring were all well tolerated and the position of the substituent groups (*ortho*-, *meta*- and *para*-) on the phenyl group had little influence on the outcome (**5a–5n**). Hetero-aromatic ketones **4o** and **4p** were also tested and the corresponding products **5o** and **5p** were both obtained in excellent conv. and ee. However, the dialkyl ketone **4q** did not work well giving the corresponding alcohol **5q** with a low ee (5% ee).

As shown in Scheme 2, a gram-scale reaction of **4a** with tiny amount of catalyst was carried out to demonstrate the potential practicability of our catalytic system. To our delight, when the

catalyst loading was decreased to 0.0005 mol% (S/C = 200,000), the transformation of acetophenone **4a** on a 2.4 g scale proceeded smoothly generating chiral alcohol **5a** with full conv. and 98% ee within 24 h at rt under a hydrogen pressure of 40 atm.

Scheme 1 Substrate Scope**Scheme 2** Gram-scale Hydrogenation of **4a**

DFT calculations were then carried out to shed light on the insight of asymmetric hydrogenation of **4a** using the novel ligand f-Amphamide **L1**.^[11] The sulfonamide can be deprotonated in the presence of the inorganic base LiO^tBu (Scheme S1).^[12] The alkali cation Li⁺ prefers to locate on the O atom of the Tosyl (Ts) group, rather than forms an alkali amidato complex as proposed in the hydrogenation mechanism by f-amphox.^[13] Possible sites for location of the added Li⁺ were examined and found that the Ir(III)-trihydride complex **I** were more stable than other isomers (Table S1 and Scheme S2). In fact, this lithium oxide successfully promotes the hydrogenation of carbonyl group. As shown in Figure 2, the catalytic cycle started by the active intermediate **I** involves (1) enantio-determining hydride transfer from Ir center of complex **I** to keto carbon of **4a** and (2) the H₂ activation process to yield **5a** and regenerate the catalyst **I**. Transition state for hydride transfer leading to (*S*)-1-phenyl ethoxide anion (**TS1(S)**) is more stable than the corresponding **TS1(R)** to (*R*)-1-phenyl ethoxide anion by 2.8 kcal/mol, which indicates 98% ee. The H₂ activation between the cationic Ir(III) and (*S*)-1-phenyl ethoxide anion incurs a barrier of 9.6 kcal/mol via **TS2(S)**.

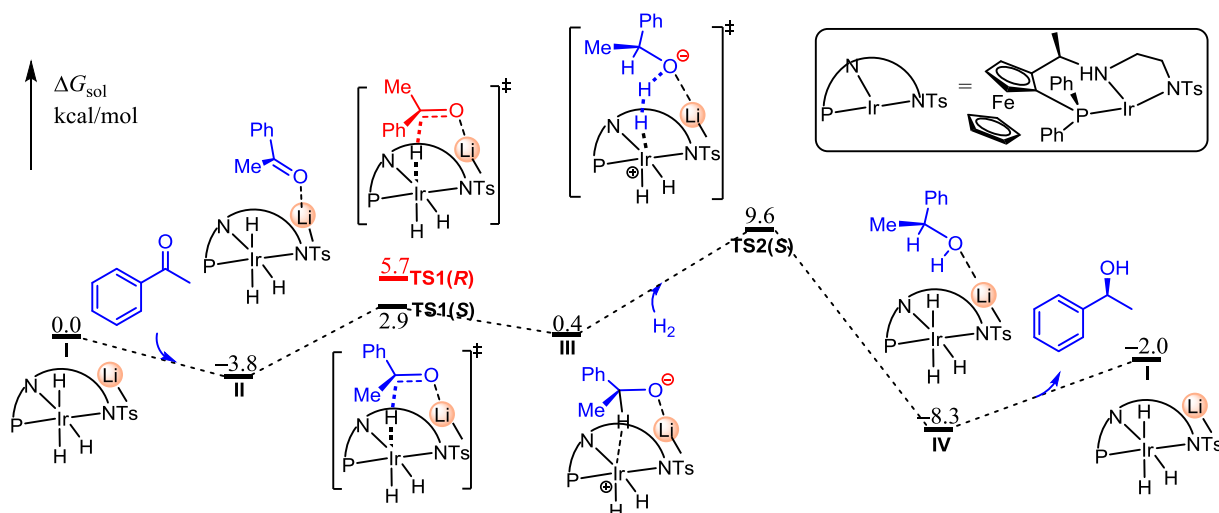


Figure 2 Gibbs Free Energy Profile for the Iridium-catalyzed Enantioselective Hydrogenation of **4a** with **L1**

The enantioselectivity is due to the more steric repulsion between Ph on P of f-Amphamide **L1** and the larger group (-Ph) of **4a** in **TS1(R)** than that in **TS1(S)**. This larger repulsion results in longer Ir-H and C-H distances in **TS1(R)** than those in **TS1(S)** (Figure 3 and Figure S1). Furthermore, the repulsion leads to better overlap between Ir-H d- σ orbital and C=O π^* orbital in HOMO-1 of **TS1(S)** than those in HOMO-1 of **TS1(R)**, showing that **TS1(S)** should be more stable than **TS1(R)**. This is consistent with the molecular orbital calculation of **TS1(S)** and **TS1(R)**. More importantly, when using ligand **L6**, even larger steric repulsion between Ar on P atom and the larger group (-Ph) of **4a** in **TS_{L6}(R)** than that in **TS_{L6}(S)** provides more obvious evidence that **TS_{L6}(S)** is more stable than **TS_{L6}(R)**. The energy difference between these two transition states is 3.1 kcal/mol, indicating an ee value of 98.9%. Our calculations are in excellent agreement with the experimental results.

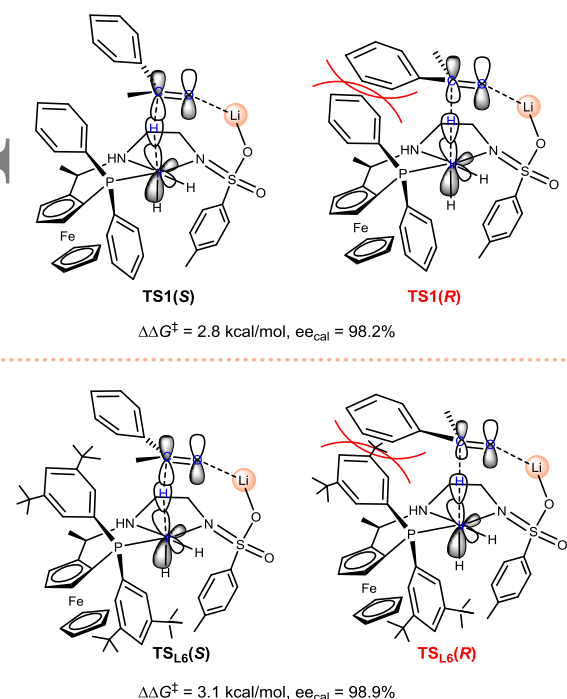


Figure 3 The Molecular Orbital Interactions and Steric Repulsions in **TS1(S)**, **TS1(R)**, **TS_{L6}(S)**, and **TS_{L6}(R)**

Conclusions

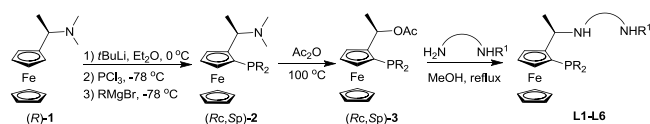
We have developed a series of novel and air-stable anionic tridentate ferrocene-based amino-phosphine sulfonamide (f-Amphamide) ligands for Ir-catalyzed enantioselective hydrogenation of simple aryl ketones. The great efficacy (TON up to 200,000) and the synthetic convenience to the novel tridentate f-Amphamide ligands make this asymmetric hydrogenation practical and user-friendly, and it should play an important role in the field of asymmetric hydrogenation. DFT calculations show that the electrophilicity of lithium oxide successfully promotes the hydrogenation of carbonyl group. Less steric repulsion in **TS1(S)** leads to better overlap between Ir-H d- σ orbital and C=O π^* orbital than that in **TS1(R)** and excellent ee values is therefore achieved. Further investigation on challenging substrates is underway and will be reported in due course.

Experimental

General remark

All reactions and manipulations which are sensitive to moisture or air were performed in an argon-filled glove box or using standard schlenk techniques. Aromatic ketones were purchased from commercial suppliers and purified by simple distillation or flash column chromatography prior to use. Anhydrous MeOH, DCM, *i*-PrOH were purchased from Sigma-Adrich. Anhydrous 1, 4-dioxane, toluene, THF, Et₂O were distilled from sodium benzophenone ketyl. Anhydrous EtOH was freshly distilled from magnesium. [Ir(COD)Cl]₂ was prepared according to the literature.^[14] ¹H NMR (400 MHz), ¹³C NMR (101 MHz) and ³¹P NMR (162 MHz) spectra were recorded on a Bruker ADVANCE III spectrometer with CDCl₃ as the solvent and tetramethylsilane (TMS) as the internal standard. Chemical shifts are reported up field to TMS (0.00 ppm) for ¹H NMR and relative to CDCl₃ (77.0 ppm) for ¹³C NMR. HRMS were recorded on APEXII and ZAB-HS spectrometer. HPLC analyses were performed using an Agilent 1260 Series instrument. GC analyses were performed using an Agilent 7890B Series instrument. GC condition : A 1 μ L portion of the extract was injected onto a 30 m X 0.25 mm X 0.25 μ m SUPELCO Beta Dex 120 capillary GC column maintained at 40 °C for 1 min, followed by a temperature gradient from 40 °C to 100 °C at 2 °C min⁻¹, a temperature gradient of 100 °C to 200 °C at 10 °C min⁻¹, injector and detector temperature was 220 °C. Column Chromatography was performed with silica gel Merck 60 (300-400 mesh).

Preparation of phosphine-amino-amide (f-Amphamide) Ligands



General procedure: To a solution of (*R*)-Ugi's amine (*R*)-1 (2.57 g, 10 mmol) in anhydrous Et₂O (20 mL) was added 1.6 M *t*BuLi solution in pentane (11.2 mmol, 7.0 mL) at 0 °C. After addition was complete, the mixture was warmed to room temperature and stirred for 2 h. The mixture was then cooled to -78 °C and fresh distilled PCl₃ (11.46 mmol, 1 mL) was added drop wise, and the mixture was warmed to room temperature overnight. The mixture was then cooled to -78 °C again, and a suspension of RMgBr (prepared from corresponding RBr (30 mmol) and magnesium turnings (0.8 g, 33.3 mmol) in THF at reflux temperature) was added slowly via cannula. After addition, the mixture was stirred overnight from -78 °C to room temperature and quenched with 20 mL saturated NH₄Cl aq. The organic layer was separated and the aqueous layer was extracted with Et₂O (3 × 20 mL). The combined organic phase was dried over Na₂SO₄ and concentrated. The residue was purified by column chromatography to afford the aminophosphine (*Rc*, *Sp*)-2 with little impurity, which was used directly in the next step without further purification.

A solution of crude aminophosphine (*Rc*, *Sp*)-2 (1 mmol) in acetic anhydride (1.5 mL) was heated to 100 °C for 1-2 h (monitored by TLC). After the starting material was disappeared, the volatiles were removed under reduced pressure. Toluene (2 mL) was then added and the resulting solution was concentrated. The operation was repeated for three times to remove excess acetic anhydride. To the residue, a small amount of *i*-PrOH or EtOH was added and the mixture was subjected to ultrasound for several minutes until the appearing of yellow solid. The alcohol was then removed by high vacuum, and the obtained yellow solid (> 95% yield) was pure enough for next step.

A mixture of the acetate (*Rc*, *Sp*)-3 (1 mmol) and corresponding amino sulfonamide^[10b] (5 mmol) in dry MeOH (5 mL) was refluxed overnight under nitrogen. The solvent was evaporated under reduced pressure to afford the crude product. After column chromatography on silica-gel column with petroleum ether/ethyl acetate (v/v = 8:1 to 5:1) as eluent, the corresponding phosphine-amino-amide (f-amphamide) Ligands were obtained as yellow solids in medium to good yields.

(L1): Yellow solid, 72% yield. [α]_D²⁰ = -247.1 (c = 1.0, CHCl₃); ¹H NMR (400 MHz, Chloroform-*d*) δ 7.65 (d, *J* = 8.3 Hz, 2H), 7.57 – 7.51 (m, 2H), 7.41 – 7.37 (m, 3H), 7.29 (d, *J* = 7.8 Hz, 2H), 7.26 – 7.14 (m, 5H), 4.42 (d, *J* = 2.3 Hz, 1H), 4.30 (t, *J* = 2.6 Hz, 1H), 4.02 (s, 5H), 4.02 – 4.00 (m, 1H), 3.85 – 3.72 (m, 1H), 2.45 (s, 3H), 2.45 – 2.42 (m, 2H), 2.29 (t, *J* = 5.4 Hz, 2H), 1.34 (d, *J* = 6.6 Hz, 3H); ¹³C {¹H} NMR (101 MHz, CDCl₃) δ 143.1, 140.0 (d, *J* = 9.9 Hz), 137.3, 136.8 (d, *J* = 8.4 Hz), 135.0, 134.8, 132.9, 132.7, 129.9, 129.6, 129.2, 128.6, 128.5, 128.4, 128.3, 128.2, 127.2, 97.0 (d, *J* = 23.1 Hz), 75.3 (d, *J* = 6.6 Hz), 71.5 (d, *J* = 4.4 Hz), 69.8, 69.3, 69.2, 69.0, 50.9 (d, *J* = 8.8 Hz), 44.6, 42.8, 21.6, 19.2; ³¹P{¹H} NMR (162 MHz, CDCl₃) δ -25.0 (s). HRMS (ESI) calcd for C₃₃H₃₆FeN₂O₂PS [M+H]⁺: 611.1579; Found: 611.1577.

(L2): Yellow solid, 41% yield. [α]_D²⁰ = -257.1 (c = 1.0, CHCl₃); ¹H NMR (400 MHz, Chloroform-*d*) δ 7.72 (d, *J* = 8.3 Hz, 2H), 7.52 – 7.48 (m, 2H), 7.44 – 7.36 (m, 3H), 7.28 (d, *J* = 3.2 Hz, 2H), 7.22 – 7.15 (m, 1H), 7.12 – 7.02 (m, 4H), 4.52 (s, 1H), 4.37 (t, *J* = 2.6 Hz, 1H), 4.08 (s, 5H), 4.04 – 4.01 (m, 1H), 3.71 (d, *J* = 1.3 Hz, 1H), 2.45 (s, 3H), 2.14 – 2.09 (m, 2H), 1.97 – 1.89 (m, 1H), 1.85 – 1.84 (m, 1H), 1.53 – 1.43 (m, 2H), 1.36 (d, *J* = 6.2 Hz, 3H), 1.08 – 1.03 (m, 2H), 0.94 – 0.76 (m, 2H); ¹³C{¹H} NMR (101 MHz, CDCl₃) δ 142.9, 140.0 (d, *J* = 10.6 Hz), 137.5, 136.8 (d, *J* = 9.5 Hz), 135.2, 135.0, 133.0, 132.8, 129.5, 129.3, 128.5, 128.5, 128.4, 128.3, 128.3, 127.6, 98.2, 74.5, 71.3 (d, *J* = 4.0 Hz), 70.6, 69.8, 69.7, 69.4, 57.9,

57.1, 46.6, 32.3, 30.0, 24.9, 24.1, 21.7, 20.2; ³¹P{¹H} NMR (162 MHz, CDCl₃) δ -24.6 (s). HRMS (ESI) calcd for C₃₇H₄₂FeN₂O₂PS [M+H]⁺: 665.2049; Found: 665.2037.

(L3): Yellow solid, 60% yield. [α]_D²⁰ = -160.9 (c = 1.0, CHCl₃); ¹H NMR (400 MHz, Chloroform-*d*) δ 7.43 – 7.41 (m, 2H), 7.35 – 7.24 (m, 8H), 7.22 – 7.16 (m, 2H), 7.05 – 6.95 (m, 3H), 6.91 – 6.90 (m, 3H), 6.84 (t, *J* = 7.4 Hz, 2H), 6.73 – 6.66 (m, 2H), 6.62 – 6.55 (m, 2H), 4.30 – 4.25 (m, 1H), 4.21 (t, *J* = 2.6 Hz, 1H), 3.93 (d, *J* = 7.5 Hz, 1H), 3.86 (s, 5H), 3.65 – 3.57 (m, 2H), 3.55 – 3.51 (m, 1H), 2.25 (s, 3H), 1.07 (d, *J* = 6.4 Hz, 3H); ¹³C{¹H} NMR (101 MHz, CDCl₃) δ 142.5, 140.7 (d, *J* = 11.0 Hz), 138.8, 137.8 (d, *J* = 9.2 Hz), 135.5, 135.3, 132.9, 132.7, 129.2, 129.0, 128.7, 128.6, 128.6, 128.3, 128.2, 128.1, 127.8, 127.8, 127.7, 127.7, 127.5, 127.3, 127.1, 98.8, 74.4 (d, *J* = 9.5 Hz), 71.6 (d, *J* = 4.0 Hz), 69.9, 69.6, 69.5, 64.9, 63.4, 47.8, 29.8, 21.6, 19.8; ³¹P{¹H} NMR (162 MHz, CDCl₃) δ -23.5 (s). HRMS (ESI) calcd for C₄₅H₄₄FeN₂O₂PS [M+H]⁺: 763.2205; Found: 763.2188

(L4): Yellow solid, 64% yield. [α]_D²⁰ = -228.2 (c = 1.0, CHCl₃); ¹H NMR (400 MHz, Chloroform-*d*) δ 7.70 (d, *J* = 8.2 Hz, 2H), 7.59 – 7.51 (m, 2H), 7.44 – 7.36 (m, 3H), 7.31 – 7.27 (m, 7H), 4.45 (s, 1H), 4.33 – 4.31 (m, 1H), 4.06 (s, 5H), 3.99 – 3.93 (m, 1H), 3.79 (s, 1H), 2.80 – 2.74 (m, 1H), 2.71 – 2.65 (m, 1H), 2.45 (s, 3H), 2.26 – 2.16 (m, 2H), 1.40 (d, *J* = 6.6 Hz, 3H), 0.97 – 0.83 (m, 2H); ¹³C{¹H} NMR (101 MHz, CDCl₃) δ 143.0, 139.8, 137.4, 135.0, 134.8, 133.1, 132.9, 129.6, 129.3, 128.8, 128.7, 128.6, 128.3, 128.3, 127.2, 97.1, 75.4, 71.4, 69.8, 69.5, 69.2, 51.7, 51.6, 45.3, 43.2, 28.2, 21.6, 19.4; ³¹P{¹H} NMR (162 MHz, CDCl₃) δ -25.4 (s). HRMS (ESI) calcd for C₃₄H₃₈FeN₂O₂PS [M+H]⁺: 625.1736; Found: 625.1734.

(L5): Yellow solid, 47% yield. [α]_D²⁰ = -171.8 (c = 1.0, CHCl₃); ¹H NMR (400 MHz, Chloroform-*d*) δ 7.56 – 7.49 (m, 2H), 7.42 – 7.36 (m, 3H), 7.26 – 7.22 (m, 2H), 7.17 (s, 2H), 7.14 – 7.06 (m, 3H), 4.87 (s, 1H), 4.41 (s, 1H), 4.29 (t, *J* = 2.5 Hz, 1H), 4.10 – 4.01 (m, 2H), 4.06 (s, 5H), 3.77 – 3.76 (m, 1H), 2.99 – 2.89 (m, 1H), 2.42 (d, *J* = 5.6 Hz, 1H), 2.31 (t, *J* = 5.4 Hz, 2H), 2.24 (t, *J* = 7.6 Hz, 1H), 1.39 (d, *J* = 6.5 Hz, 3H), 1.30 (d, *J* = 7.0 Hz, 6H), 1.23 (t, *J* = 6.8 Hz, 12H). ¹³C{¹H} NMR (101 MHz, CDCl₃) δ 152.4, 150.4, 134.9, 134.7, 133.1, 132.9, 129.2, 128.8, 128.5, 128.4, 128.3, 128.3, 123.8, 100.1, 75.5 (d, *J* = 6.5 Hz), 71.4 (d, *J* = 4.2 Hz), 69.9, 69.3 (d, *J* = 3.7 Hz), 69.0, 50.9, 50.8, 44.4, 42.5, 34.3, 29.6, 25.1 (d, *J* = 2.6 Hz), 23.8 (d, *J* = 2.9 Hz), 19.2. ³¹P{¹H} NMR (162 MHz, CDCl₃) δ -25.3 (s). HRMS (ESI) calcd for C₄₁H₅₂FeN₂O₂PS [M+H]⁺: 723.2831; Found: 723.2816.

(L6): Yellow solid, 54% yield. [α]_D²⁰ = -183.1 (c = 1.0, CHCl₃); ¹H NMR (400 MHz, Chloroform-*d*) δ 7.64 (d, *J* = 8.3 Hz, 2H), 7.47 – 7.38 (m, 3H), 7.28 – 7.26 (m, 3H), 7.24 – 7.18 (m, 2H), 4.36 (s, 1H), 4.26 (t, *J* = 2.7 Hz, 1H), 4.06 (s, 5H), 3.99 – 3.92 (m, 1H), 3.70 (s, 1H), 2.43 (s, 3H), 2.41 – 2.35 (m, 1H), 2.12 – 2.05 (m, 3H), 1.31 (s, 18H), 1.29 (d, *J* = 6.5 Hz, 3H), 1.18 (s, 18H). ¹³C{¹H} NMR (101 MHz, CDCl₃) δ 150.8 (d, *J* = 7.3 Hz), 150.4 (d, *J* = 7.3 Hz), 143.1, 138.2, 137.6, 135.0 (d, *J* = 7.0 Hz), 129.7, 129.1, 128.9, 128.0, 128.8, 127.2, 123.1, 122.8, 96.2 (d, *J* = 23.0 Hz), 77.4, 71.2 (d, *J* = 4.1 Hz), 69.8, 69.1 (d, *J* = 3.4 Hz), 68.6, 51.1, 51.0, 44.9, 42.8, 35.1, 34.9, 31.6, 31.5, 21.6, 19.3. ³¹P{¹H} NMR (162 MHz, CDCl₃) δ -24.4 (s). HRMS (ESI) calcd for C₄₉H₆₈FeN₂O₂PS [M+H]⁺: 835.4083; Found: 835.4067

Procedure for asymmetric hydrogenation of ketones

General procedure for S/C = 10 000: To a 2.5 mL vial was added the catalyst precursor [Ir(COD)Cl]₂ (3.4 mg, 0.005 mmol), ligand L6 (9.2 mg, 0.011 mmol) and anhydrous *i*-PrOH (2.0 mL) under argon atmosphere. The mixture was stirred for 1 h at room temperature to give a clear yellow solution. An aliquot of the catalyst solution (20 μ L, 0.0002 mmol) was transferred into a 5 mL hydrogenation vessel, LiO^{*t*}Bu (1.6 mg), ketone (2 mmol) and anhydrous *i*-PrOH (2 mL) was added. The vessels were placed in an autoclave which was then charged with 20 atm of H₂ and stirred at 25-30 °C for 12 h. After slowly releasing the hydrogen

pressure, the reaction mixture was passed through a short column of silica gel to remove the metal complex. The product was analyzed by ¹H NMR to determine the conversion. The ee values were determined by HPLC analysis on a chiral stationary phase.

(S)-1-phenylethanol (5a): $[\alpha]_D^{20} = -59.7$ ($c = 1.0$, CHCl₃), > 99% conversion, 98% ee. The enantiomeric excess was determined by HPLC on Chiralcel OD-H column, hexane: isopropanol = 95:5; flow rate = 1.0 mL/min; UV detection at 210 nm; $t_R = 7.5$ min (minor), $t_R = 8.6$ min (major), ¹H NMR (400 MHz, CDCl₃) δ 7.49 (dd, $J = 10.7$, 4.4 Hz, 1H), 7.26 – 7.22 (m, 1H), 7.16 (t, $J = 7.4$ Hz, 1H), 7.09 – 6.95 (m, 1H), 7.08 – 6.88 (m, 1H), 5.19 (dd, $J = 9.6$, 4.8 Hz, 1H), 2.57 (d, $J = 15.8$, 10.4 Hz, 1H), 1.51 (d, $J = 6.5$ Hz, 3H).^[5]

(S)-1-phenylpropan-1-ol (5b): $[\alpha]_D^{20} = -48.7$ ($c = 1.0$, CHCl₃), > 99% conversion, 99% ee. The enantiomeric excess was determined by HPLC on Chiralcel OJ-H column, hexane: isopropanol = 95:5; flow rate = 1.0 mL/min; UV detection at 210 nm; $t_R = 8.7$ min (major), $t_R = 9.3$ min (minor), ¹H NMR (400 MHz, CDCl₃) δ 7.44 – 7.33 (m, 4H), 7.34 – 7.22 (m, 1H), 4.62 (t, $J = 6.6$ Hz, 1H), 1.92 (d, $J = 13.4$ Hz, 1H), 1.90 – 1.70 (m, 2H), 0.94 (t, $J = 7.4$ Hz, 3H).

(S)-1-(p-tolyl)ethanol (5c): $[\alpha]_D^{20} = -52.1$ ($c = 1.0$, CHCl₃), > 99% conversion, 99% ee. The enantiomeric excess was determined by HPLC on Chiralcel OJ-H column, hexane: isopropanol = 95:5; flow rate = 1.0 mL/min; UV detection at 210 nm; $t_R = 11.9$ min (minor), $t_R = 10.6$ min (major), ¹H NMR (400 MHz, CDCl₃) δ 7.29 (t, $J = 6.6$ Hz, 2H), 7.19 (d, $J = 7.9$ Hz, 2H), 4.89 (q, $J = 6.1$ Hz, 1H), 2.37 (s, 3H), 1.88 (s, 1H), 1.51 (d, $J = 6.4$ Hz, 3H).

(S)-1-(4-methoxyphenyl)ethanol (5d): $[\alpha]_D^{20} = -41.7$ ($c = 1.0$, CHCl₃), > 99% conversion, 97% ee. The enantiomeric excess was determined by HPLC on Chiralcel OJ-H column, hexane: isopropanol = 95:5; flow rate = 1.0 mL/min; UV detection at 230 nm; $t_R = 18.1$ min (major), $t_R = 19.3$ min (minor), ¹H NMR (400 MHz, CDCl₃) δ 7.32 (d, $J = 8.4$ Hz, 2H), 6.91 (d, $J = 8.3$ Hz, 2H), 4.87 (q, $J = 6.4$ Hz, 1H), 3.83 (s, 3H), 1.91 (s, 1H), 1.50 (d, $J = 6.4$ Hz, 3H).

(S)-1-(3-methoxyphenyl)ethanol (5e): $[\alpha]_D^{20} = -44.0$ ($c = 1.0$, CHCl₃), > 99% conversion, 99% ee. The enantiomeric excess was determined by HPLC on Chiralcel OJ-H column, hexane: isopropanol = 95:5; flow rate = 1.0 mL/min; UV detection at 210 nm; $t_R = 14.1$ min (major), $t_R = 15.9$ min (minor), ¹H NMR (400 MHz, CDCl₃) δ 7.29 (dd, $J = 10.0$, 6.1 Hz, 1H), 7.00 – 6.92 (m, 2H), 6.84 (dd, $J = 8.1$, 1.9 Hz, 1H), 4.89 (q, $J = 6.4$ Hz, 1H), 3.84 (s, 3H), 2.06 (s, 1H), 1.51 (d, $J = 6.5$ Hz, 3H).

(S)-1-(2-fluorophenyl)ethanol (5f): $[\alpha]_D^{20} = -52.1$ ($c = 1.0$, CHCl₃), > 99% conversion, 99% ee. The enantiomeric excess was determined by HPLC on Chiralcel OJ-H column, hexane: isopropanol = 98:2; flow rate = 1.0 mL/min; UV detection at 210 nm; $t_R = 6.9$ min (major), $t_R = 14.2$ min (minor), ¹H NMR (400 MHz, CDCl₃) δ 7.54 – 7.49 (m, 1H), 7.29 – 7.24 (m, 1H), 7.18 (t, $J = 7.4$ Hz, 1H), 7.09 – 7.00 (m, 1H), 5.23 (d, $J = 6.1$ Hz, 1H), 1.98 (s, 1H), 1.55 (d, $J = 6.5$ Hz, 3H).

(S)-1-(3-fluorophenyl)ethanol (5g): $[\alpha]_D^{20} = -42.5$ ($c = 1.0$, CHCl₃), > 99% conversion, 99% ee. The enantiomeric excess was determined by HPLC on Chiralcel OD-H column, hexane: isopropanol = 95:5; flow rate = 1.0 mL/min; UV detection at 210 nm; $t_R = 12.6$ min (major), $t_R = 13.1$ min (minor), ¹H NMR (400 MHz, CDCl₃) δ 7.39 – 7.24 (m, 1H), 7.20 – 7.07 (m, 2H), 7.00 – 6.96 (m, 1H), 4.92 (q, $J = 6.4$ Hz, 1H), 2.00 (s, 1H), 1.51 (d, $J = 6.5$ Hz, 3H).

(S)-1-(2-chlorophenyl)ethanol (5h): $[\alpha]_D^{20} = -56.8$ ($c = 1.0$, CHCl₃), > 99% conversion, 99% ee. The enantiomeric excess was determined by HPLC on Chiralcel OJ-H column, hexane: isopropanol = 95:5; flow rate = 1.0 mL/min; UV detection at 210 nm; $t_R = 7.6$ min (major), $t_R = 8.1$ min (minor), ¹H NMR (400 MHz, CDCl₃) δ 7.62 – 7.60 (m, 1H), 7.35 – 7.30 (m, 2H), 7.29 – 7.20 (m, 1H), 5.31 (q, $J = 6.4$ Hz, 1H), 2.25 (s, 1H), 1.51 (d, $J = 6.4$ Hz, 3H).

(S)-1-(3-chlorophenyl)ethanol (5i): $[\alpha]_D^{20} = -40.4$ ($c = 1.0$,

CHCl₃), > 99% conversion, 96% ee. The enantiomeric excess was determined by HPLC on Chiralcel OJ-H column, hexane: isopropanol = 95:5; flow rate = 1.0 mL/min; UV detection at 210 nm; $t_R = 9.0$ min (major), $t_R = 10.2$ min (minor), ¹H NMR (400 MHz, CDCl₃) δ 7.40 (s, 1H), 7.33 – 7.23 (m, 3H), 4.89 (q, $J = 6.4$ Hz, 1H), 2.02 (s, 1H), 1.50 (d, $J = 6.5$ Hz, 3H).

(S)-1-(4-chlorophenyl)ethanol (5j): $[\alpha]_D^{20} = -49.4$ ($c = 1.0$, CHCl₃), > 99% conversion, 97% ee. The enantiomeric excess was determined by HPLC on Chiralcel OJ-H column, hexane: isopropanol = 95:5; flow rate = 1.0 mL/min; UV detection at 210 nm; $t_R = 9.0$ min (major), $t_R = 9.5$ min (minor), ¹H NMR (400 MHz, CDCl₃) δ 7.39 – 7.23 (m, 4H), 4.87 (q, $J = 6.4$ Hz, 1H), 2.27 (s, 1H), 1.47 (d, $J = 6.5$ Hz, 3H).

(S)-1-(2-bromophenyl)ethanol (5k): $[\alpha]_D^{20} = -40.4$ ($c = 1.0$, CHCl₃), > 99% conversion, 96% ee. The enantiomeric excess was determined by HPLC on Chiralcel OJ-H column, hexane: isopropanol = 95:5; flow rate = 1.0 mL/min; UV detection at 210 nm; $t_R = 7.7$ min (major), $t_R = 8.2$ min (minor), ¹H NMR (400 MHz, CDCl₃) δ 7.61 (dd, $J = 7.8$, 1.4 Hz, 1H), 7.53 (d, $J = 8.0$ Hz, 1H), 7.36 (t, $J = 7.5$ Hz, 1H), 7.17 – 7.13 (m, 1H), 5.25 (q, $J = 6.3$ Hz, 1H), 2.25 (s, 1H), 1.50 (d, $J = 6.4$ Hz, 3H).

(S)-1-(4-bromophenyl)ethanol (5l): $[\alpha]_D^{20} = -46.2$ ($c = 1.0$, CHCl₃), > 99% conversion, 96% ee. The enantiomeric excess was determined by HPLC on Chiralcel OD-H column, hexane: isopropanol = 95:5; flow rate = 1.0 mL/min; UV detection at 230 nm; $t_R = 7.5$ min (major), $t_R = 8.0$ min (minor), ¹H NMR (400 MHz, CDCl₃) δ 7.52 – 7.47 (m, 2H), 7.28 (t, $J = 4.2$ Hz, 2H), 4.90 (q, $J = 6.1$ Hz, 1H), 1.84 (s, 1H), 1.50 (d, $J = 6.5$ Hz, 3H).

(S)-1-(4-(trifluoromethyl)phenyl)ethanol (5m): $[\alpha]_D^{20} = -36.8$ ($c = 1.0$, CHCl₃), > 99% conversion, 97% ee. The enantiomeric excess was determined by HPLC on Chiralcel OJ-H column, hexane: isopropanol = 95:5; flow rate = 1.0 mL/min; UV detection at 230 nm; $t_R = 6.7$ min (major), $t_R = 7.1$ min (minor), ¹H NMR (400 MHz, CDCl₃) δ 7.63 (d, $J = 8.1$ Hz, 2H), 7.51 (d, $J = 8.0$ Hz, 2H), 4.98 (d, $J = 6.3$ Hz, 1H), 2.04 (d, $J = 9.1$ Hz, 1H), 1.53 (d, $J = 6.5$ Hz, 3H).

(S)-1-(naphthalen-2-yl)ethanol (5n): $[\alpha]_D^{20} = -52.9$ ($c = 1.0$, CHCl₃), > 99% conversion, >99% ee. The enantiomeric excess was determined by HPLC on Chiralcel OJ-H column, hexane: isopropanol = 95:5; flow rate = 1.0 mL/min; UV detection at 210 nm; $t_R = 27.7$ min (major), $t_R = 36.6$ min (minor), ¹H NMR (400 MHz, CDCl₃) δ 7.94 – 7.74 (m, 4H), 7.59 – 7.44 (m, 3H), 5.07 (q, $J = 6.4$ Hz, 1H), 2.21 (s, 1H), 1.60 (d, $J = 6.5$ Hz, 3H).

(S)-1-(thiophen-2-yl)ethanol (5o): $[\alpha]_D^{20} = -26.6$ ($c = 1.0$, CHCl₃), > 99% conversion, 96% ee. The enantiomeric excess was determined by HPLC on Chiralcel OJ-H column, hexane: isopropanol = 95:5; flow rate = 1.0 mL/min; UV detection at 250 nm; $t_R = 10.0$ min (major), $t_R = 12.2$ min (minor), ¹H NMR (400 MHz, CDCl₃) δ 7.38 – 7.18 (m, 1H), 7.08 – 6.87 (m, 2H), 5.20 – 5.11 (m, 1H), 2.08 (s, 1H), 1.63 (d, $J = 6.4$ Hz, 3H).

(S)-1-(furan-2-yl)ethanol (5p): $[\alpha]_D^{20} = -45.3$ ($c = 1.0$, CHCl₃), > 99% conversion, 92% ee. The enantiomeric excess was determined by HPLC on Chiralcel OJ-H column, hexane: isopropanol = 95:5; flow rate = 1.0 mL/min; UV detection at 210 nm; $t_R = 8.6$ min (major), $t_R = 9.5$ min (minor), ¹H NMR (400 MHz, CDCl₃) δ 7.39 (s, 1H), 6.34 (s, 1H), 6.24 (d, $J = 3.0$ Hz, 1H), 4.89 (q, $J = 6.5$ Hz, 1H), 2.22 (s, 1H), 1.56 (d, $J = 6.6$ Hz, 3H).

(S)-heptan-2-ol (5q): $[\alpha]_D^{20} = -2.5$ ($c = 1.0$, CHCl₃), > 99% conversion, 5% ee (by GC). The enantiomeric excess was determined by GC after acylation on β -dex 120, $t_R = 28.5$ min (minor), $t_R = 30.3$ min (major), ¹H NMR (400 MHz, CDCl₃) δ 3.80 (q, $J = 6.0$ Hz, 1H), 1.52 – 1.23 (m, 8H), 1.19 (d, $J = 6.2$ Hz, 3H), 0.89 (t, $J = 6.8$ Hz, 3H).

Asymmetric hydrogenation of acetophenone at S/C = 200,000: To a 2.5 mL vial was added the catalyst precursor [Ir(COD)Cl]₂ (3.4 mg, 0.005 mmol), ligand **L6** (8.5 mg, 0.011 mmol) and anhydrous *i*-PrOH (1 mL) under argon atmosphere. The mixture was stirred for 1 h at room temperature to give a clear

yellow solution. An aliquot of the catalyst solution (10 μ L, 0.0001 mmol) was transferred into a 10 mL hydrogenation vessel, then a solution of LiO^tBu (0.8 mg, 0.01 mmol), acetophenone (20 mmol) and anhydrous *i*-PrOH (1.5 mL) was added. The vessel was placed in an autoclave which was then charged with 40 atm of H₂ and stirred at 25-30 °C for 24 h. The work-up was identical to that described for the asymmetric hydrogenation at S/C = 10,000. (S)-1-Phenylethanol (**5a**): > 99% conversion, 98% ee (S).

Supporting Information

The supporting information for this article is available on the WWW under <https://doi.org/10.1002/cjoc.2018xxxxx>.

Acknowledgement (optional)

This work was supported by a start-up fund from Southern University of Science and Technology (to X. Zhang), Shenzhen Science and Technology Innovation Committee (KQTD20150717103157174, to X. Zhang) and National Natural Science Foundation of China (No. 21573102, to L. Dang). We greatly acknowledge the referees for their helpful suggestions on the mechanistic studies.

References

- [1] (a) Zhao, M. M.; McNamara, J. M.; Ho, G. J.; Emerson, K. M.; Song, Z. J.; Tschäen, D. M.; Brands, K. M. J.; Dolling, U.; Grabowski, E. J. J.; Reider, P. J. *J. Org. Chem.* **2002**, *67*, 6743. (b) Tang, W.; Zhang, X. *Chem. Rev.* **2003**, *103*, 3029. (c) Creighton, C. J.; Ramabadrán, K.; Ciccone, P. E.; Liu, J.; Orsini, M. J.; Reitz, A. B. *Bioorg. Med. Chem. Lett.* **2004**, *14*, 4083. (d) Rogawski, M. A.; Loscher, W. *Nat Rev Neurosci* **2004**, *5*, 553. (e) Almeida, L.; Soares-da-Silva, P. *Neurotherapeutics* **2007**, *4*, 88. (f) Hagmann, W. K. J. *Med. Chem.* **2008**, *51*, 4359. (g) Cui, J. J.; Tran-Dubé, M.; Shen, H.; Nambu, M.; Kung, P.-P.; Pairish, M.; Jia, L.; Meng, J.; Funk, L.; Botrous, I.; McTigue, M.; Grodsky, N.; Ryan, K.; Padriqué, E.; Alton, G.; Timofeevski, S.; Yamazaki, S.; Li, Q.; Zou, H.; Christensen, J.; Mroczkowski, B.; Bender, S.; Kania, R. S.; Edwards, M. P. *J. Med. Chem.* **2011**, *54*, 6342. (h) Xie, J.-H.; Bao, D.-H.; Zhou, Q.-L. *Synthesis* **2015**, *47*, 460. (i) Jiang, W.; Zhao, Q.; Tang, W. *Chin. J. Chem.* **2018**, *36*, 153. (j) Zhang, Z.; Andrew, B. N.; Zhou, M.; Liu, D.; Zhang, W. *Chin. J. Chem.* **2018**, *36*, 443.
- [2] (a) Noyori, R.; Ohkuma, T. *Angew. Chem., Int. Ed.* **2001**, *40*, 40. (b) Ohkuma, T.; Sandoval, C. A.; Srinivasan, R.; Lin, Q.; Wei, Y.; Muñiz, K.; Noyori, R. *J. Am. Chem. Soc.* **2005**, *127*, 8288. (c) Le Roux, E.; Malacea, R.; Manoury, E.; Poli, R.; Gonsalvi, L.; Peruzzini, M. *Adv. Synth. Catal.* **2007**, *349*, 309. (d) Irrgang, T.; Friedrich, D.; Kempe, R. *Angew. Chem., Int. Ed.* **2011**, *50*, 2183. (e) Xie, J.-B.; Xie, J.-H.; Liu, X.-Y.; Zhang, Q.-Q.; Zhou, Q.-L. *Chem. - Asian J.* **2011**, *6*, 899. (f) Puylaert, P.; van Heck, R.; Fan, Y.; Spannenberg, A.; Baumann, W.; Beller, M.; Medlock, J.; Bonrath, W.; Lefort, L.; Hinze, S.; de Vries, J. G. *Chem.-Eur. J.* **2017**, *23*, 8473. (g) Vasilenko, V.; Blasius, C. K.; Wadepohl, H.; Gade, L. H. *Angew. Chem., Int. Ed.* **2017**, *56*, 8393. (h) Wang, M.-H.; Chen, L.-Y. *Tetrahedron Lett.* **2017**, *58*, 732.
- [3] (a) Ohkuma, T.; Ooka, H.; Hashiguchi, S.; Ikariya, T.; Noyori, R. *J. Am. Chem. Soc.* **1995**, *117*, 2675. (b) Noyori, R.; Hashiguchi, S. *Acc. Chem. Res.* **1997**, *30*, 97. (c) Doucet, H.; Ohkuma, T.; Murata, K.; Yokozawa, T.; Kozawa, M.; Katayama, E.; England, A. F.; Ikariya, T.; Noyori, R. *Angew. Chem., Int. Ed.* **1998**, *37*, 1703. (d) Ohkuma, T.; Koizumi, M.; Doucet, H.; Pham, T.; Kozawa, M.; Murata, K.; Katayama, E.; Yokozawa, T.; Ikariya, T.; Noyori, R. *J. Am. Chem. Soc.* **1998**, *120*, 13529.
- [4] (a) Jiang, Y.; Jiang, Q.; Zhang, X. *J. Am. Chem. Soc.* **1998**, *120*, 3817. (b) Burk, M. J.; Hems, W.; Herzberg, D.; Malan, C.; Zanotti-Gerosa, A. *Org. Lett.* **2000**, *2*, 4173. (c) Henschke, J. P.; Burk, M. J.; Malan, C. G.; Herzberg, D.; Peterson, J. A.; Wildsmith, A. J.; Copley, C. J.; Casy, G. *Adv. Synth. Catal.* **2003**, *345*, 300. (d) Xie, J.-H.; Wang, L.-X.; Fu, Y.; Zhu, S.-F.; Fan, B.-M.; Duan, H.-F.; Zhou, Q.-L. *J. Am. Chem. Soc.* **2003**, *125*, 4404. (e) Hu, A.; Ngo, H. L.; Lin, W. *Org. Lett.* **2004**, *6*, 2937. (f) Hedberg, C.; Källström, K.; Arvidsson, P. I.; Brandt, P.; Andersson, P. G. *J. Am. Chem. Soc.* **2005**, *127*, 15083. (g) Ohkuma, T.; Utsumi, N.; Tsutsumi, K.; Murata, K.; Sandoval, C.; Noyori, R. *J. Am. Chem. Soc.* **2006**, *128*, 8724. (h) Ohkuma, T.; Tsutsumi, K.; Utsumi, N.; Arai, N.; Noyori, R.; Murata, K. *Org. Lett.* **2007**, *9*, 255. (i) Li, W.; Sun, X.; Zhou, L.; Hou, G.; Yu, S.; Zhang, X. *J. Org. Chem.* **2009**, *74*, 1397. (j) Li, W.; Hou, G.; Wang, C.; Jiang, Y.; Zhang, X. *Chem. Commun.* **2010**, *46*, 3979. (k) Phillips, S. D.; Fuentes, J. A.; Clarke, M. L. *Chem.-Eur. J.* **2010**, *16*, 8002. (l) Touge, T.; Hakamata, T.; Nara, H.; Kobayashi, T.; Sayo, N.; Saito, T.; Kayaki, Y.; Ikariya, T. *J. Am. Chem. Soc.* **2011**, *133*, 14960. (m) Jolley, K. E.; Zanotti-Gerosa, A.; Hancock, F.; Dyke, A.; Grainger, D. M.; Medlock, J. A.; Nedden, H. G.; Le Paih, J. J. M.; Roseblade, S. J.; Seger, A.; Sivakumar, V.; Prokes, I.; Morris, D. J.; Wills, M. *Adv. Synth. Catal.* **2012**, *354*, 2545. (n) Yamamura, T.; Nakatsuka, H.; Tanaka, S.; Kitamura, M. *Angew. Chem., Int. Ed.* **2013**, *52*, 9313. (o) Bao, D.-H.; Wu, H.-L.; Liu, C.-L.; Xie, J.-H.; Zhou, Q.-L. *Angew. Chem., Int. Ed.* **2015**, *54*, 8791.
- [5] Xie, J.-H.; Liu, X.-Y.; Xie, J.-B.; Wang, L.-X.; Zhou, Q.-L. *Angew. Chem., Int. Ed.* **2011**, *50*, 7329.
- [6] (a) Nie, H.; Zhou, G.; Wang, Q.; Chen, W.; Zhang, S. *Tetrahedron: Asymmetry* **2013**, *24*, 1567. (b) Tomoya, Y.; Hiroshi, N.; Shinji, T.; Masato, K. *Angew. Chem., Int. Ed.* **2013**, *52*, 9313. (c) Widegren, M. B.; Harkness, G. J.; Slawin, A. M. Z.; Cordes, D. B.; Clarke, M. L. *Angew. Chem., Int. Ed.* **2017**, *56*, 5825.
- [7] Wu, W.; Liu, S.; Duan, M.; Tan, X.; Chen, C.; Xie, Y.; Lan, Y.; Dong, X.-Q.; Zhang, X. *Org. Lett.* **2016**, *18*, 2938.
- [8] Yu, J.; Long, J.; Yang, Y.; Wu, W.; Xue, P.; Chung, L. W.; Dong, X.-Q.; Zhang, X. *Org. Lett.* **2017**, *19*, 690.
- [9] Yu, J.; Duan, M.; Wu, W.; Qi, X.; Xue, P.; Lan, Y.; Dong, X.-Q.; Zhang, X. *Chem.-Eur. J.* **2017**, *23*, 970.
- [10] (a) Dijkstra, A.; Elzinga, J. M.; Li, Y.-X.; Arends, I. W. C. E.; Sheldon, R. A. *Tetrahedron: Asymmetry* **2002**, *13*, 879. (b) Abdel-Maksoud, M. S.; Kim,

M.-R.; El-Gamal, M. I.; Gamal El-Din, M. M.; Tae, J.; Choi, H. S.; Lee, K.-T.; Yoo, K. H.; Oh, C.-H. *Eur. J. Med. Chem.* **2015**, *95*, 453.

[11] Calculations were conducted by using Gaussian 09 program package. Geometries used were optimized in the gas phase with B3LYP functional. The solvation effects in iPrOH were simulated using the PCM solvent model at B3LYP-D3/6-311++G** level. Please see the computational details in Supporting Information.

[12] (a) John, J. M.; Takebayashi, S.; Dabral, N.; Miskolzie, M.; Bergens, S. *H. J. Am. Chem. Soc.* **2013**, *135*, 8578. (b) Dub, P. A.; Henson, N. J.; Martin, R. L.; Gordon, J. C. *J. Am. Chem. Soc.* **2014**, *136*, 3505. (c) Hayes, J. M.; Deydier, E.; Ujaque, G.; Lledós, A.; Malacea-Kabbara, R.; Manoury, E.; Vincendeau, S.; Poli, R. *ACS Catal.* **2015**, *5*, 4368. (d) Dub, P. A.; Gordon, J. C. *Dalton Transactions* **2016**, *45*, 6756. (e) Dub, P. A.; Gordon, J. C. *ACS Catal.* **2017**, 6635.

[13] (a) Gu, G.; Yang, T.; Yu, O.; Qian, H.; Wang, J.; Wen, J.; Dang, L.; Zhang, X. *Org. Lett.* **2017**, *19*, 5920. (b) Gu, G.; Yang, T.; Lu, J.; Wen, J.; Dang, L.; Zhang, X. *Org. Chem. Front.* **2018**, *5*, 1209.

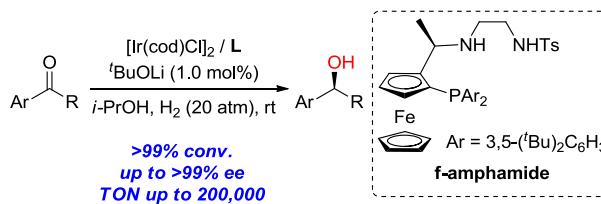
[14] (a) Choudhury, J.; Podder, S.; Roy, S. *J. Am. Chem. Soc.* **2005**, *127*, 6162. (b) Yang, D.; Long, Y.; Wang, H.; Zhang, Z. *Org. Lett.* **2008**, *10*, 4723.

[15] (a) Nie, H.; Yao, L.; Li, B.; Zhang, S.; Chen, W. *Organometallics* **2014**, *33*, 2109. (b) Gischig, S.; Togni, A. *Organometallics* **2004**, *23*, 2479. (c) Chen, W.; Mbafor, W.; Roberts, S. M.; Whittall, J. *J. Am. Chem. Soc.* **2006**, *128*, 3922. (d) Hu, X.-P.; Chen, H.-L.; Zheng, Z. *Adv. Synth. Catal.* **2005**, *347*, 541. (e) Zhou, Z. M.; Zhang, Y. M. *Synth. Commun.* **2005**, *35*, 2401.

Entry for the Table of Contents

Page No.

**Scope and Mechanism on
Iridium-f-Amphamide Catalyzed
Asymmetric Hydrogenation of Ketones**



A series of novel and easily accessed ferrocene-based amino-phosphine-sulfonamide (f-Amphamide) ligands have been developed and applied in Ir-catalyzed asymmetric hydrogenation of aryl ketones, affording the corresponding chiral secondary alcohols with excellent results (up to >99% conversion, >99% ee and TON up to 200,000). DFT calculations suggest an activating model involving an alkali cation Li⁺.

Zhi-Qin Liang, Ti-Long Yang, Guoxian Gu, Li Dang* and Xumu Zhang*
